J Polym Res (2013) 20:213
DOI 10.1007/s10965-013-0213-6

ORIGINAL PAPER

A new low band gap donor–acceptor alternating copolymer containing dithienothiophene and fluorenone unit

Tzong-Liu Wang · Yeong-Tarng Shieh · Chien-Hsin Yang · Yan-Yu Chen · Tsung-Han Ho · Chin-Hsiang Chen

Received: 26 March 2013 / Accepted: 7 July 2013 / Published online: 20 July 2013

Abstract A low bandgap copolymer poly(3,5-didecanyldi thieno[3,2-b:2′,3′-d]thiophene-*alt*-9-fluorenone) (PDTTFO) consisting of dithieno[3,2-b:2′,3′-d]thiophene (DTT) and 9-fluorenone (FO) was synthesized as the donor material for the polymer solar cells via Stille coupling polymerization. Both donor and acceptor units were confirmed by FT-IR and ^{1}H-NMR. Optoelectronic properties of the PDTTFO copolymer were investigated and observed by UV-vis, photolumi nescence (PL) spectrum, and cyclic voltammogram (CV). UV-vis spectrum of the film exhibited two absorption peaks centered at 358, 474 nm with a broad absorption band in the range of 300–700 nm and showed a low bandgap of 1.68 eV. The highest occupied molecular orbital (HOMO) and lowest unoccupied molecular orbital (LUMO) energy levels of the polymer were estimated to be −5.09 and −3.41 eV, respectively. Based on the ITO/PEDOT:PSS/PDTTFO:PCBM/Al device structure, the power conversion efficiency (PCE) under the illumination of AM 1.5 (100 mW/cm^2) was 0.374 %. The effects of annealing temperature on the device performance were studied. At annealing temperature of 175 °C/30 min, the device demonstrated an optimal efficiency of 0.923 %. The improved device efficiency under the optimal condition was confirmed by the higher light harvest in UV-vis spectra, the enhanced quenching of photoluminescence (PL) emission, the improved nanoscale morphology by atomic force microscopy (AFM) examination, and the increase in external quantum efficiency.

Keywords Low bandgap · Conjugated polymers · Donor–acceptor copolymer · Power conversion efficiency · Annealing

T.-L. Wang (✉) · Y.-T. Shieh · C.-H. Yang · Y.-Y. Chen
Department of Chemical and Materials Engineering, National University of Kaohsiung, Kaohsiung 811, Taiwan, Republic of China
e-mail: tlwang@nuk.edu.tw

T.-H. Ho
Department of Chemical and Materials Engineering, National Kaohsiung University of Applied Sciences, Kaohsiung 807, Taiwan, Republic of China

C.-H. Chen
Department of Electronic Engineering, Cheng Shiu University, Kaohsiung 833, Taiwan, Republic of China

Introduction

In recent decades, polymer solar cells (PSCs) based on conjugated polymers have attracted considerable attention due to their unique advantages and great potential for future cheap and renewable energy applications, such as low cost solution fabrication process, large areas, light weight and practicability in flexible devices [1–4]. Efficient polymer-based solar cells utilize donor-electron acceptor bulk heterojunction (BHJ) films as active layers [5, 6]. Among the various electron donor conjugated polymers, the most commonly used one is regioregular poly(3-hexylthiophene) (P3HT), and the generally used electron acceptor is the fullerene derivative [6, 6]-phenyl C_{61} butyric acid methyl ester ($PC_{61}BM$) owing to their good electron-accepting and electron-transporting properties. So far, BHJ photovoltaic devices combining P3HT with PCBM normally could achieve power conversion efficiencies (PCEs) of 4~6 % [7–9], and some of reported BHJ blends from intermixed polymeric donors and fullerene acceptors have reached an even higher PCE exceeding 8 % [7]. However, even though polymer-based BHJ solar cells have achieved quite respectable power conversion efficiencies, there still remain several questions that will limit the device performance. For instance, the relatively large bandgap of P3HT will result in the mismatch of the absorption spectrum of the active layer and the solar emission, especially in the red and near-infrared region, where the wavelength of solar photons that offer major energy. The hole mobility in the polymer

component and the nanoscale morphology of the active layer will also affect the further enhancement of cell performance [8–13].

In this paper, we aim at improving the PCE of the organic photovoltaic (OPV) devices by finding new conjugated polymer donor materials with broader absorption, lower bandgap, higher hole mobility, and suitable electronic energy levels to maximize the J_{sc} and V_{oc}. For designing low bandgap polymers for application in PSCs, the concept of donor–acceptor (D–A) type copolymers is promising because of the vast possibility in the unit combinations which can tailor the energy levels of conjugated polymer [14–17]. Through the introduction of push-pull driving forces to facilitate electron delocalization and the formation of quinoid mesomeric structures over the conjugated main chain, the bond length alternation (BLA) can be significantly reduced. The bandgap decreases linearly as a function of the increasing quinoid character with concomitant decreasing BLA value [18, 19]. The electronic and optoelectronic properties of donor–acceptor copolymers could be efficiently manipulated by controlling intramolecular charge transfer (ICT) which is correlated with the high-lying HOMO of the donor unit and the low-lying LUMO of the acceptor unit [19, 20]. Many D–A type copolymers have been used in PSCs to achieve PCEs above 5 % with extensive device engineering efforts [14, 21–23].

Well-chosen D and A groups are particularly desirable for low band gap polymers. In the design of D–A type conjugated polymers, one of the most useful strategies is to introduce the monomer unit with highly planar nature and stable quinoid form into the polymer backbone to enhance π-conjugation and reduce the band gap [24]. Fused aromatic ring moieties are well known for these kinds of characters [25–28]. Due to the rigidity and planarity, π-extended heteroarene structure makes the polymer backbone more rigid and coplanar, and therefore enhances strong π–π stacking interaction. Charge carriers are expected to transport efficiently not only along the polymer chain but also through intermolecular hopping in the π–π direction [26, 29, 30], therefore leading to a high hole mobility of the copolymer with lower bandgap, extending absorption, and good electrochemical stability [31–33]. Recently, some of representative polymer systems containing fused thiophene units have demonstrated efficiencies greater than 7 % [34–37], which shows a very attractive feature for high-performance OPV devices.

Dithieno[3,2-*b*:2′,3′-*d*]thiophene (DTT) is a fused thiophene units that have been widely used in organic field-effect transistors (OTFTs) application [34–38]. It is also one of the popular units in fused thiophene ring system due to the great possibility they have showed in recent reports. Most DTT-containing copolymers exhibited high crystallinity, charge carrier mobility and excellent environmental stability, which are attributed to the highly extended heteroarene structure of DTT to offer better electron-donating properties [30, 38–40]. Furthermore, several reports have showed high PCEs over 5 % by using DTT as a building block [30, 41], that make us paid a great attention to DTT units and its electric and optical properties.

On the other hand, 9-fluorenone (FO) is an acceptor type compound with the structure of a flat fused ring, which is useful in constructions of low bandgap polymers. FO is advantageous as an acceptor unit because it can be directly incorporated into the D–A type copolymer without introducing steric effects into the polymer backbone. In addition, 2,7-dibromo-9-fluorenone is an inexpensive and a commercially available product which could be used in the Stille coupling reaction of D–A type copolymer without tedious synthetic steps.

Since both building blocks have the structure of flat and fused ring, it was expected that a low bandgap polymer with a high hole mobility and strong absorption ability could be obtained for this type of D–A copolymer. Herein, we have synthesized a new copolymer consisting of alternating DTT and FO units via the Stille coupling reaction, where the DTT unit has attached two alkyl chains to increase the solubility. The optoelectronic properties and the PCEs of the fabricated PSCs were investigated. The effect of thermal annealing on the PCEs of solar cells is also reported.

Experimental

Materials

Tetrabromothiophene (Alfa Aesar), n-butyllithium (Acros), undecanal (Alfa Aesar), sodium bichromate (SHOWA), ethyl mercaptoacetate (Acros), potassium carbonate (SHOWA), lithium hydroxide (Alfa Aesar), copper (Alfa Aesar), bis(triphenylphosphine)palladium(II) dichloride ($Pd(PPh_3)Cl_2$, Alfa Aesar), 2,7-dibromo-9-fluorenone (TCI), poly(3,4-ethylene dioxythiophene)-poly(styrenesulfonate) (PEDOT:PSS, Aldrich), phenyl-C_{61}-butyric acid methyl ester ($PC_{61}BM$, FEM Tech.) were used as received. All other reagents were used as received.

Synthesis

The donor material, 3,5-didecanyldithieno[3,2-*b*:2′,3′-*d*]thiophene (DTT), was prepared via the approaches similar to the published procedures [42–46]. The acceptor material, 9-fluorenone (FO) was obtained from the commercial product: 2,7-dibromo- 9-fluorenone. The copolymer poly(3,5-dideca nyldithieno [3,2-b:2′,3′-d]thiophene-*alt*-9-fluorenone) (PDTT FO) was synthesized via Stille coupling reaction of the donor unit of 2,6-bis-trimethylatannanyl (3,5-didecanyldithieno)[3,2-*b*:2′,3′-*d*]thiophene with the acceptor unit of 2,7-dibromo-9-fluorenone.

Preparation of 2,6-bis-trimethylstannanyl (3,5-didecanyldithieno[3,2-*b*:2′,3′-*d*]thiophene)

To a solution of 3,5-didecanyldithieno[3,2-*b*:2′,3′-*d*]thiophene (0.56 mmole) in THF (20 mL), n-BuLi (0.8 ml,1.6 M in hexanes) was added dropwise at −78 °C under argon. The reaction was keep at −78 °C for 2 h. Then $ClSn(Me)_3$ (1.2 ml) was added. The reaction mixture was warmed to room temperature and reacted for another 10 h. The reaction was quenched by adding 60 mL of water and the organic layer was separated. The aqueous layer was extracted with diethyl ether three times and then dried over with anhydrous $MgSO_4$. After purified by column chromatography using toluene as eluent, the product was given as viscous brown oil. The synthetic route is shown in Scheme 1. Yield: 39 %. ^1H NMR (500 MHz, $CDCl_3$, δ ppm): 2.37 (t, 4H), 1.83 (m, 4H), 1.25 (m, 28H), 0.88 (t, 6H), 0.27 (s, 18H, Sn-CH_3).

Synthesis of D–A type copolymer (PDTTFO)

In a 250 mL flask, the two monomers (1 mmol of each), 2,6-bis-trimethylstannanyl (3,5-didecanyldithieno)[3,2-*b*:2′,3′-*d*]thiophene and 2,7-dibromo-9-fluorenone were dissolved in 20 mL of dry DMF and then flushed by argon for 10 min. Following that, 0.03 mmol of $Pd(PPh_3)Cl_2$ was added, and the reactant was purged by argon for another 20 min. The reaction mixture was then heated at 120 °C for 72 h under the protection of argon. The solution was cooled and poured into 100 mL of methanol, where the crude polymer was precipitated and collected as powder, which was then subjected to Soxhlet extraction with methanol for 2–3 days. The polymer was recovered from the THF fraction by rotary evaporation. The synthetic route is shown in Scheme 1. Yield: 57 %. ^1H NMR (500 MHz, $CDCl_3$, δ ppm): 7.97 (t, 2H), 7.74 (m, 2H), 7.51 (m,1H), 7.35 (m,1H), 2.42 (t, 4H), 1.85 (m, 4H), 1.29–1.31 (m, 28H), 0.88 (t, 6H). Anal. Calcd for $(C_{41}H_{48}OS_3)_n$: C, 75.41; H, 7.41. Found: C, 76.58; H, 7.64. GPC (THF): $\overline{Mn} = 9,100 g/mol$, $\overline{Mw} = 12,800 g/mol$, PDI=1.41.

Device fabrication and characterization

The device structure of the polymer photovoltaic cells in this study is ITO/PEDOT:PSS/PDTTFO:$PC_{61}BM$/Al. Before device fabrication, the glass substrates coated with indium tin oxide (ITO) were first cleaned by ultrasonic treatment in acetone, detergent, de-ionized water, methanol and isopropyl alcohol sequentially. The ITO surface was spin coated with ca. 80 nm layer of poly(3,4-ethylene dioxythiophene): poly(styrene) (PEDOT:PSS) in the nitrogen-filled glove-box. The substrate was dried for 10 min at 150 °C and then continued to spin coating the active layer. The PDTTFO:$PC_{61}BM$ blend solutions were prepared with 1:1 weight ratio (10 mg/mL PDTTFO) in 1,2-dichlorobenzene (DCB) as the active layer. The obtained thickness for the blend film of PDTTFO:$PC_{61}BM$ was ca. 115 nm. The devices were completed by evaporation of metal electrodes Al with area of 6 mm^2 defined by masks.

The films of active layers were annealed directly on top of a hot plate in the glove box, and the temperature was monitored

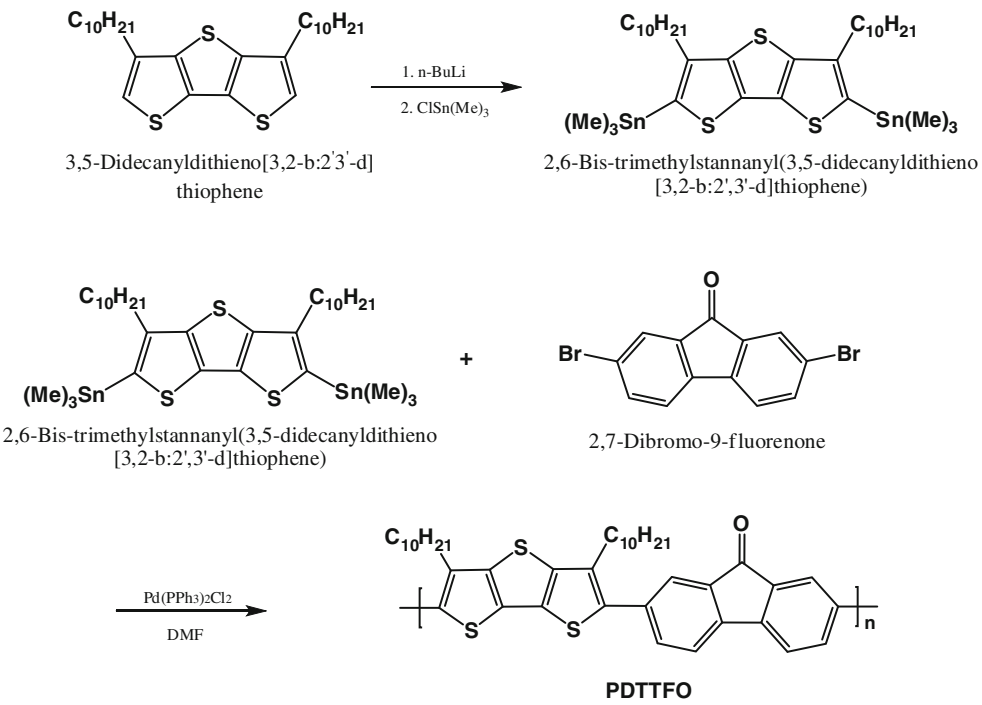

Scheme 1 Synthesis of PDTTFO copolymer

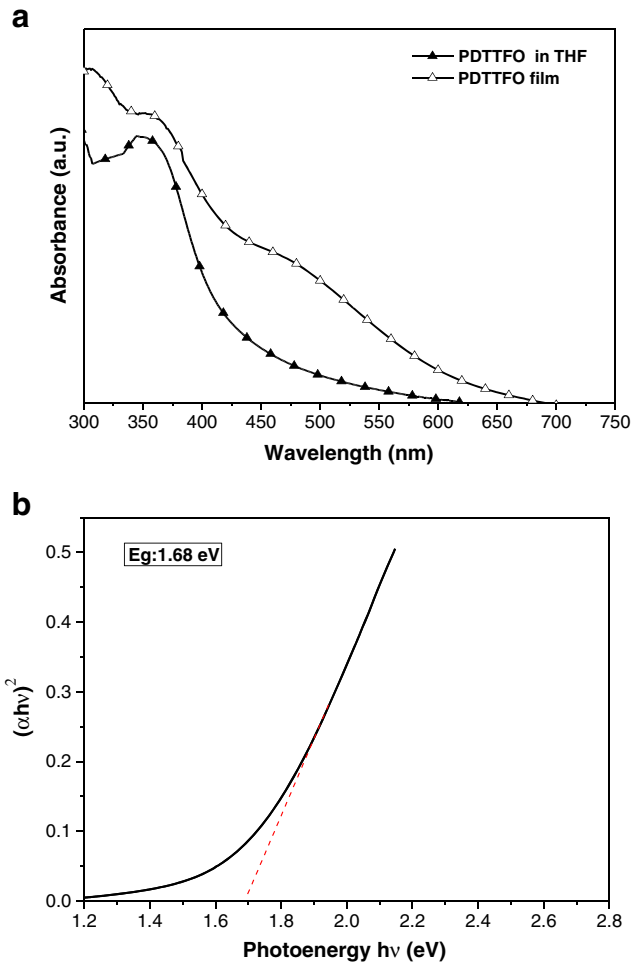

Fig. 1 **a** UV-vis absorption spectra of PDTTFO in dilute THF solution and thin film, **b** Plot of $(\alpha h\nu)^2$ vs. $h\nu$ for PDTTFO film

by using a thermocouple touching the top of the substrates. After removal from the hotplate, the substrates were immediately put onto a metal plate at room temperature. Ultraviolet-visible (UV-vis) spectroscopic analysis was conducted on a Perkin–Elmer Lambda 35 UV-vis spectrophotometer. Photoluminescence (PL) spectrum was recorded on a Hitachi F-7000 fluorescence spectrophotometer. After removing Al electrode, the film topography images of active layers were recorded with a Digital Instruments Dimension 3100 atomic force microscope (AFM) in tapping mode under ambient conditions. The J-V curves were measured under illumination from a solar simulator, using a Keithley 2400 source meter. The intensity of solar simulator was set with a primary reference cell and a spectral correction factor to give the performance under the AM 1.5 (100 mW/cm^2)

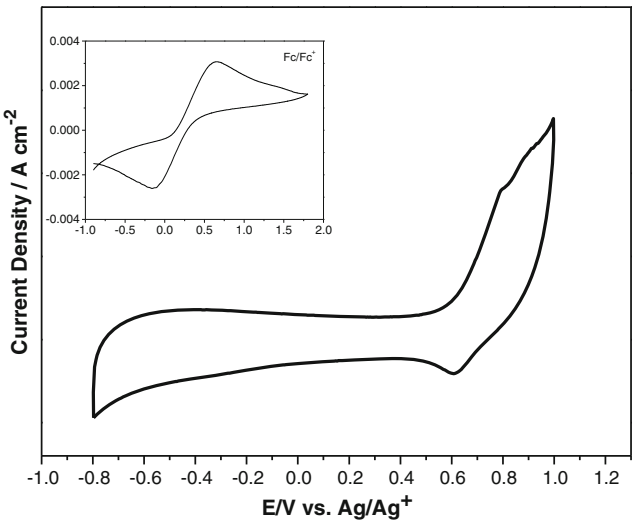

Fig. 3 Cyclic voltammograms of PDTTFO film on an ITO substrate in CH_3CN/AcOH (V/V=7/1) containing 0.1 M tetrabutylammonium perchlorate at a scan rate of 50 mVs^{-1}

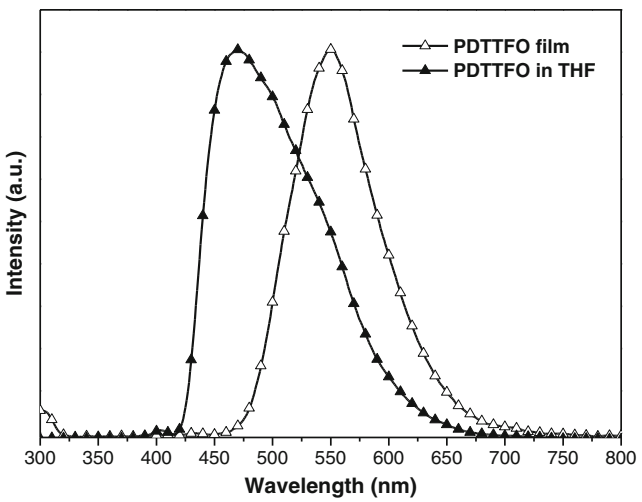

Fig. 2 Photoluminescence spectra of PDTTFO in dilute THF solution and thin film with excitation at 300 nm

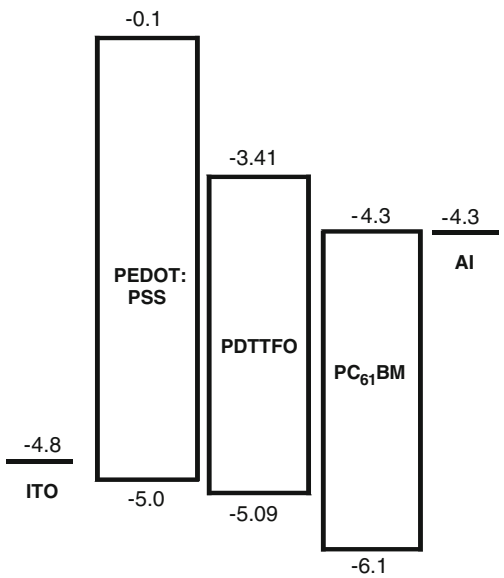

Fig. 4 Energy level diagram of the components in the polymer solar cell

Table 1 Photovoltaic characteristics of devices for the PDTTFO:$PC_{61}BM$ blend under different annealing temperatures for 30 min

	RT	100 °C	125 °C	150 °C	175 °C	200 °C
V_{oc} (V)	0.208	0.258	0.205	0.298	0.282	0.287
J_{sc} (mA/cm^2)	6.409	7.464	10.28	8.942	9.303	7.374
FF (%)	28.03	30.74	26.80	32.63	35.11	31.90
η (%)	0.374	0.592	0.565	0.869	0.923	0.675

global reference spectrum (IEC 60904-9). EQE was detected with a QE-3000 (Titan Electro-Optics Co., Ltd.) lock-in amplifier under monochromatic illumination. Calibration of the incident light was performed with a monocrystalline silicon diode. Mobility measurements were performed using an Agilent 4155C parameter analyzer.

Results and discussion

Synthesis and characterization

Since the completely flat crystal structure of dithieno[3,2-*b*:2′,3′-*d*]thiophene (DTT) enhance a good π-conjugation across the fused ring, we have synthesized a new D–A type copolymer containing the DTT segment as the donor unit and another flat fused ring of 9-fluorenone (FO) as the acceptor unit in this study. In addition, in comparison with regioregular poly(3-alkylthiophene)s, PDTTs are polymers with extended conjugation and show high charge carrier delocalization and reduced bandgaps [47, 48]. Therefore, we expected that a low bandgap D–A type copolymer would be obtained to facilitate the power conversion efficiency of solar cells.

The synthetic route toward the polymer is outlined in Scheme 1. The polymer is well dissolved in common organic solvents such as chloroform, 1,2-dichlorobenzene, THF, and toluene. In addition, the polymer exhibited a high glass transition temperature (T_g) of 152 °C as a result of the rigid donor and acceptor units.

Optical properties

Figure 1a shows the absorption spectra of the PDTTFO copolymer in dilute THF solution and in thin solid film. The spectrum of the PDTTFO film exhibits a broad absorption ranging from 300 to 700 nm. The optical absorption threshold at 706 nm of red light region from the spectrum of the film corresponds to the bandgap (E_g) of the PDTTFO copolymer. Hence, the estimated optical bandgap is 1.76 eV. To obtain a more accurate optical bandgap of PDTTFO, the fundamental equation $\alpha h\nu = B(h\nu - E_{opt})^n$ developed in Tauc relation was used [49]. As shown in Fig. 1b, the optical bandgap calculated by this equation is 1.68 eV. Both estimated optical bandgap (E_g^{opt}) and curve-fitting optical bandgap (E_g^{opt} by Tauc relation) are far smaller than that (E_g^{opt} =1.9 eV) of the widely used regioregular P3HT.

As seen from Fig. 1a, the UV-vis absorption spectrum of the copolymer in dilute THF solution exhibits a smaller absorption band ranging from UV region to 620 nm with one absorption peak positioned at about 356 nm. The solid-state absorption spectrum of PDTTFO shows a bathochromic shift compared to that of the polymer in THF solution with two absorption peaks centered at 358 and 474 nm, respectively. The former one is due to the π–π* transition of the dithienothiophene moiety [50], while the last peak is assigned to the intramolecular charge transfer (ICT) between the donor and the acceptor [51]. The small red-shift indicates more efficient π-stacking and stronger intermolecular interactions in the solid state. In particular, the broadened absorption spectrum extended to 700 nm reveals that a low bandgap polymer has been obtained,

Table 2 Photovoltaic characteristics of devices for the PDTTFO:$PC_{61}BM$ blend prepared at various weight ratios

Ratio (w/w)	1:1	1:1.5	1:2	1:2.5
V_{oc} (V)	0.208	0.229	0.251	0.197
J_{sc} (mA/cm^2)	6.409	7.691	7.922	6.388
FF (%)	28.03	28.55	31.59	32.49
η (%)	0.374	0.502	0.628	0.409

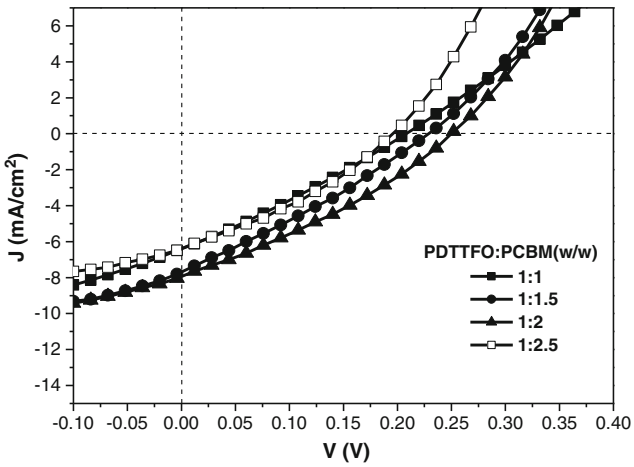

Fig. 5 J-V characteristics of devices under AM 1.5 simulated solar illumination at an intensity of 100 mW/cm^2 for the PDTTFO:$PC_{61}BM$ blend prepared at various weight ratios

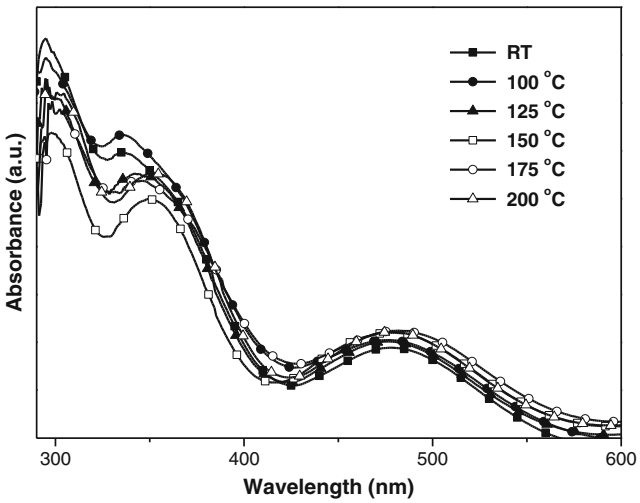

Fig. 6 UV-vis absorption spectra of PDTTFO:$PC_{61}BM$ blend films after annealing at different temperatures for 30 min

as evident from the E_g of PDTTFO. It is apparent that the ICT interaction between donor and acceptor moieties in D–A copolymers is a practical approach to lower the bandgap and broaden the absorption bands of conjugated polymers. Hence, our successful synthesis of a low bandgap D–A type copolymer is further confirmed.

The photoluminescence (PL) emission spectra of PDTTFO in dilute THF solution and thin film are shown in Fig. 2. Both the fluorescence spectra exhibit the vibronic structure with a maximum at 470 and 550 nm, respectively. As seen from the figure, both spectra show only one emission peak, indicating that an effective energy transfer from the DTT segments to the FO unit occurs. The red-shift in the spectrum of the PDTTFO film is probably due to the lowering of bandgap of copolymer by more efficient π-stacking in the solid state.

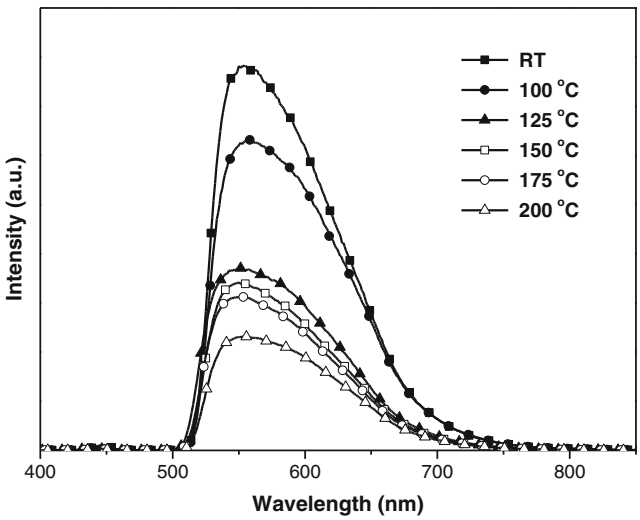

Fig. 7 Photoluminescence spectra of PDTTFO:$PC_{61}BM$ blend films after annealing at different temperatures for 30 min with excitation at 300 nm

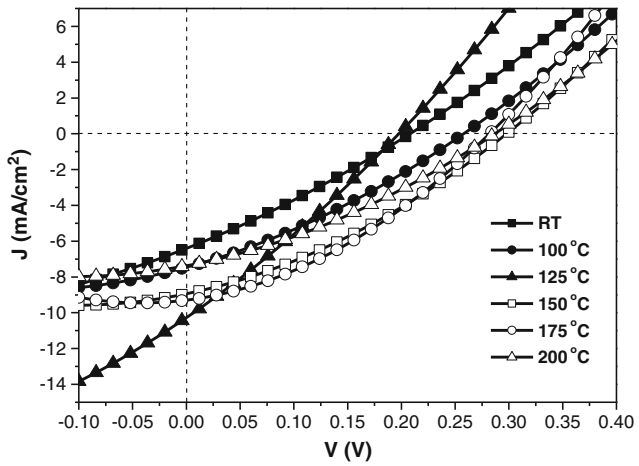

Fig. 8 J-V characteristics of devices under AM 1.5 simulated solar illumination at an intensity of 100 mW/cm^2 after annealing at different temperatures for 30 min

Electrochemical properties and energy levels

Cyclic voltammetry (CV) is a preliminary characterization technique to determine the redox properties of organic and polymeric materials. The HOMO energy level can be calculated from the onset oxidation potential [E_{ox}(onset)] based on the reference energy level of ferrocene (4.8 eV below the vacuum level, which is defined as zero) according to Eq. (1). The LUMO level can be obtained from Eq. (2) based on the E_g from Fig. 1. E_{FC} is the potential of the internal standard, the ferrocene/ferrocenium (Fc/Fc^+) redox couple.

$$\mathrm{HOMO} = -[E_{ox}(\mathrm{onset}) - E_{FC} + 4.8]\mathrm{eV} \quad (1)$$

$$\mathrm{LUMO} = \mathrm{HOMO} + E_g \quad (2)$$

As seen in Fig. 3, the E_{ox}(onset) for PDTTFO has been determined as 0.54 V vs. Ag/Ag^+. E_{FC} is 0.25 V vs. Ag/Ag^+. Hence, the HOMO energy for PDTTFO has been evaluated to be −5.09 eV and the LUMO level determined from Eq. (2) is −3.41 eV. Figure 4 shows the schematic diagram representing the potential metrically determined HOMO and LUMO energy of PDTTFO and $PC_{61}BM$ relative to the work function of the electrodes.

Device characteristics

The bulk heterojunction solar cells based on PDTTFO in combination of $PC_{61}BM$ has been prepared for investigation of device characteristics. The employed device structure was ITO/PEDOT:PSS/PDTTFO:$PC_{61}BM$/Al. The blend solutions (in DCB) of PDTTFO:$PC_{61}BM$ were prepared with 1:1 weight ratio as the active layer. The photovoltaic performance of the device for the blend film cast at room temperature (RT) was measured under illumination from solar simulator at

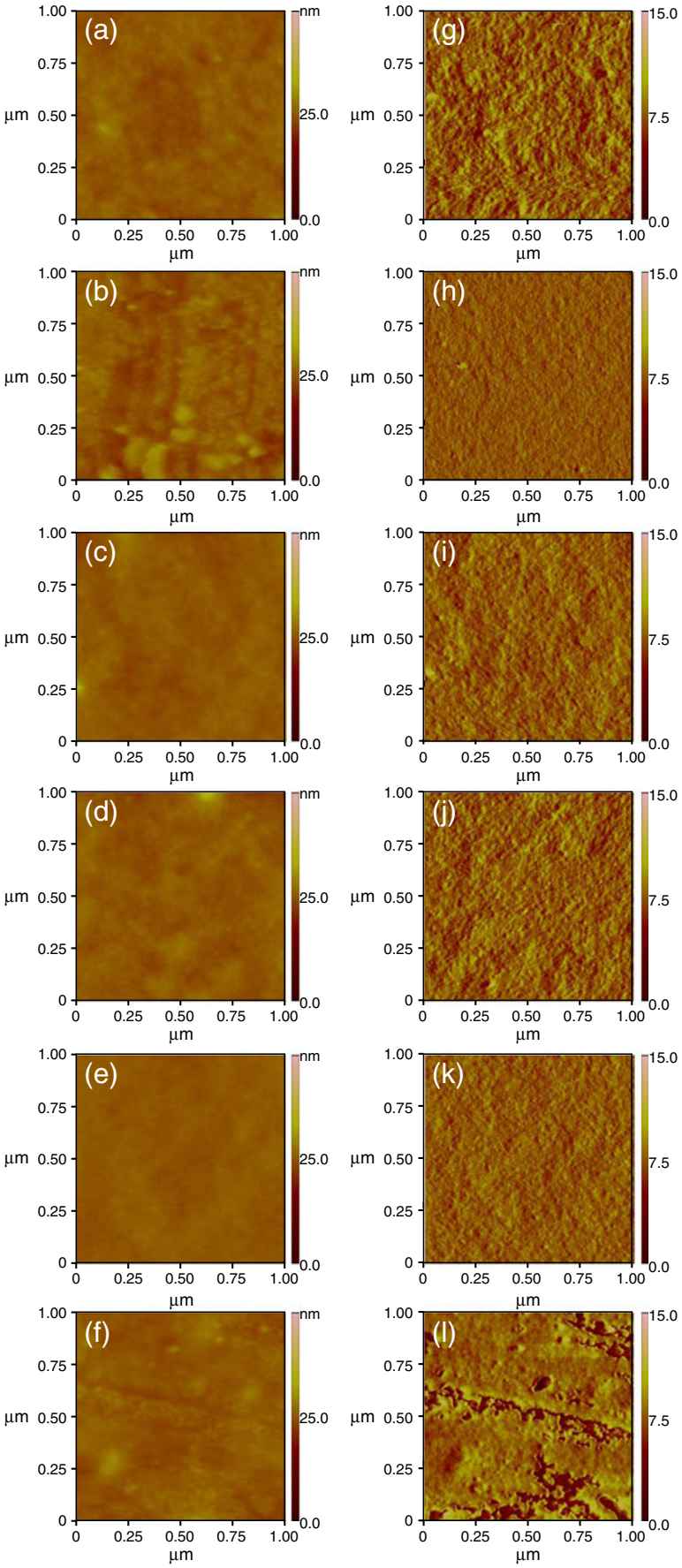

Fig. 9 AFM topography images (1×1 µm) of PDTTFO:$PC_{61}BM$ blend films after annealing at different temperatures for 30 min. 2D height image for the blend film **a** unannealed, **b** annealed at 100 °C, **c** annealed at 125 °C, **d** annealed at 150 °C, **e** annealed at 175 °C, and **f** annealed at 200 °C. Phase image for the blend film **g** unannealed, **h** annealed at 100 °C, **i** annealed at 125 °C, **j** annealed at 150 °C, **k** annealed at 175 °C, and **l** annealed at 200 °C

Table 3 Surface roughness of PDTTFO:$PC_{61}BM$ blend films obtained from AFM after annealing at different temperatures for 30 min

Annealing temp.	RT	100 °C	125 °C	150 °C	175 °C	200 °C
Average roughness (nm)	0.434	0.643	0.745	0.832	1.226	0.748
Root Mean Square (nm)	0.541	0.865	0.953	1.078	1.589	1.018

100 mW/cm^2 light intensity. The corresponding open-circuit voltage (V_{oc}), short-circuit current (J_{sc}), fill factor (FF), and power conversion efficiency (PCE,η) are listed in Table 1. The power conversion efficiency of the solar cell using the as-prepared blend film as the active layer is 0.374 %, which didn't show the expected result, though it exhibited a good J_{sc} value. The low efficiency may be due to the low V_{oc} (0.208 V) which is arising from the high-lying HOMO (−5.09 eV), the low FF (0.280), a result of the lower molecular weight of polymer ($\overline{Mn} = 9,100 \mathrm{g/mol}$), non-optimized morphology of the blend film, etc. However, because the PL emission of the PDTTFO/$PC_{61}BM$ blend was not completely quenched at the weight ratio of 1:1, the photovoltaic performances of PSCs based on the higher $PC_{61}BM$ contents were also measured. The results are shown in Table 2 and Fig. 5. It was found that J_{sc} increased significantly with the increase of the $PC_{61}BM$ content from a blend ratio of 1:1 to 1:2. However, J_{sc} decreased at the ratio of 1:2.5 presumably because of increased aggregation of $PC_{61}BM$ [27]. Thus, the optimal device efficiency was obtained from the device with a blend of PDTTFO and $PC_{61}BM$ at a weight ratio of 1:2. For the blend ratio of 1:2, the obtained values of J_{sc} and PCE are 7.922 mA/cm^2 and 0.628 %, respectively.

Thermal annealing

Thermal annealing is an effective way to elevate the photovoltaic performance of polymer solar cells. The effect of annealing temperature on the UV-vis absorption spectra for the thin films of PDTTFO:$PC_{61}BM$ (1:1 weight ratio) spun cast on quartz substrates is shown in Fig. 6. The annealing time was kept at 30 min for all annealing temperatures.

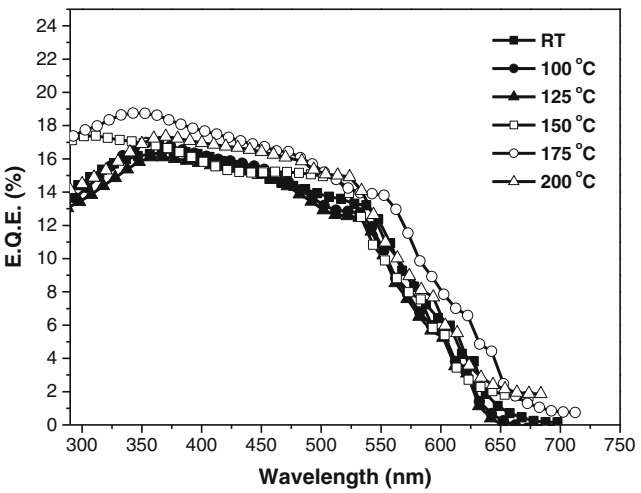

Fig. 10 EQE spectra of PDTTFO:$PC_{61}BM$ blend films after annealing at different temperatures for 30 min

As seen in Fig. 6, all of the spectra of the annealed samples show three absorption bands. An increase in the absorption strength after heat treatment normally means increased packing of the PDTTFO domains. Most of maximum absorption bands are observed for the film annealed at 175 °C, indicating an enhanced conjugation length and a more ordered structure of PDTTFO. Since the thickness of all the films is similar (ca. 115 nm), the increase in the peak absorption intensity during thermal annealing may be attributed to the lowering of the bandgap between π and π*, the increase of the optical π–π* transition, and the increased interchain interaction among the PDTTFO. After thermal annealing, the PDTTFO molecules afford higher energy and move more easily. Consequently, the polymer chains become mobile and self-organization can occur to form ordering. Therefore, the peak intensity increases in the more ordered films due to the improved charge carrier transport in both donor (PDTTFO) and acceptor ($PC_{61}BM$) phases after thermal annealing. Further increasing the annealing temperature to 200 °C, however, results in a decrease in the intensities of the three bands. From these results, in order to obtain the highest power conversion efficiency the optimum annealing temperatures for PDTTFO and $PC_{61}BM$ may be around 175 °C.

Figure 7 shows the PL intensity for blend films annealed at different temperatures. The PL is due to photogenerated excitons in PDTTFO that do not take part in charge separation. PL quenching provides direct evidence for exciton dissociation, and thus efficient PL quenching is necessary to obtain efficient organic solar cells. As shown in the figure, it can be seen that the PL intensity decreases with the increase of annealing temperature. The significant reduction in the PL intensity is attributed to efficient photoinduced charge separation between electron-donating (PDTTFO) and electron-accepting ($PC_{61}BM$) molecules. The PL intensity shows a minimum at the annealing temperature of 200 °C. This may be attributed to the higher charge carrier mobility or the higher interfacial area between D–A molecules as compared with those of other annealing temperatures. However, this does not necessarily mean that the stronger the PL quenching is, the better the performance of the solar cells is. Although the PL intensity of the blend film annealed at 175 °C is higher in comparison with that of the film annealed

at 200 °C, the highest power conversion efficiency (0.923 %) is achieved by this blend film as shown in Fig. 8 and Table 1.

Since the morphology of heterojunction plays an important role on the performance of polymer solar cells, the topographies of blend films of PDTTFO:$PC_{61}BM$ (1:1, w/w) were studied by AFM. The 2D height images and phase images of film surfaces at different annealing temperatures have been taken and shown in Fig. 9. The values of average roughness and root-mean-square roughness for the blend films by AFM are shown in Table 3. As seen from the phase images in Fig. 9, compared to the films annealed at other temperatures, both PDTTFO and $PC_{61}BM$ domains of the film annealed at 175 °C are more uniformly distributed throughout the surface of the film, indicating the nanoscale interpenetrating network has been formed in this blend, which can benefit not only the charge separation but also the charge transport. In addition, it is evident from the height images and Table 3 that a rougher surface was observed in the film annealed at 175 °C. As mentioned in several literatures [52–55], a rougher surface will increase the contact area between the active layer and the metal electrode in a blend film. Thus, this will enhance the transport rate of charge carriers to the metal electrode while reducing the charge recombination of the excitons. Therefore, the highest PCE for the film annealed at 175 °C could be justified since it possesses the highest values of roughness. Moreover, the fact that the highest PCE is acquired by this film is further confirmed below.

External quantum efficiency and solar cell performance

The external quantum efficiency (EQE) for photocurrent is the number of electrons flowing per second in the external circuit of a solar cell divided by the number of photons per second of a specific energy (or wavelength) that enter the solar cell. This measurement is often also referred to as IPCE. The acronym IPCE stands for incident photon (to charge) conversion efficiency. In order to learn more on the recombination mechanisms in the PDTTFO/$PC_{61}BM$ photoactive layer, EQE measurements with monochromatic wave from 290 to 700 nm were performed on the solar cell devices (Fig. 10).

As seen in the figure, the EQE spectra of blend films exhibit similar patterns with the optical data. For the untreated sample, a dominant band present at 376 nm with an EQE of 16.4 %. After thermal treatment for the blend films, the EQE is significantly improved with minor changes in the peak position. Among the EQE spectra taken from different annealing temperatures, the film annealed at 175 °C almost demonstrates the highest EQE in the most illuminated regions by possessing the EQE of the dominant band reaching ca. 19 %. Consequently, the highest power conversion efficiency (0.923 %) has been achieved by this blend film. However, the EQE values are still small compared to those of high performance PSCs. The low EQE may be attributed to the high recombination rate of charge carriers in the PDTTFO/$PC_{61}BM$ blend system, which results in the low photocurrent.

Conclusions

The D–A type copolymer PDTTFO based on DTT and FO units has been synthesized and employed as the donor material in the active layer of BHJ-type polymer solar cells. UV-vis absorption spectra indicated that an expected low bandgap polymer with a wide absorption band has been obtained. Through the annealing treatment at an optimum condition (175 °C/30 min), the photovoltaic performance was significantly improved and the power conversion efficiency of the device reached 0.923 % under white light illumination (100-mW/cm^2). We attribute the higher efficiency to the improved morphology in the active layer, increase of light absorption, and higher carrier mobility.

Acknowledgments We gratefully acknowledge the support of the National Science Council of Republic of China with Grant NSC 99-2221-E-390-001-MY3.

References

1. Krebs FC, Jorgensen M, Norrman K, Hagemann O, Alstrup J, Nielsen TD, Fyenbo J, Larsen K, Kristensen J (2009) Sol Energy Mater Sol Cells 93:422
2. Krebs FC (2009) Sol Energy Mater Sol Cells 93:465
3. Krebs FC, Gevorgyan SA, Alstrup J (2009) J Mater Chem 19:5442
4. Nielsen TD, Cruickshank C, Foged S, Thorsen J, Krebs FC (2010) Sol Energy Mater Sol Cells 94:1553
5. Inganäs O, Svensson M, Zhang F, Gadisa A, Persson NK, Wang X, Andersson MR (2004) J Appl Phys A 79:31
6. Zhang F, Mammo W, Andersson LM, Admassie S, Andersson MR, Inganäs O (2006) Adv Mater 18:2169
7. Green MA, Emery K, Hishikawa Y, Warta W, Dunlop ED (2011) Prog Photovolt Res Appl 19:565
8. Ma W, Yang C, Gong X, Lee K, Heeger AJ (2005) Adv Funct Mater 15:1617
9. Yang X, Van Duren JKJ, Rispens MT, Hummelen JC, Janssen RAJ, Michels MAJ, Loos J (2004) Adv Mater 16:802
10. Savenije TJ, Kroeze JE, Yang X, Loos J (2005) Adv Funct Mater 15:1260
11. Bavel V, Sourty SS, De With E, Loos GJ (2009) Nano Lett 9:507
12. Coffey DC, Reid OG, Rodovsky DB, Bartholomew GP, Ginger DS (2007) Nano Lett 7:738
13. Chu C, Yang H, Hou W, Huang J, Li G, Yang Y (2008) Appl Phys Lett 92:103306
14. Peet J, Kim JY, Coates NE, Ma WL, Moses D, Heeger AJ, Bazan GC (2007) Nat Mater 6:497
15. Wang EG, Wang L, Lan LF, Luo C, Zhuang WL, Peng JB, Cao Y (2008) Appl Phys Lett 92:033307/1
16. Zhan X, Tan Z, Domercq B, An Z, Zhang X, Barlow S, Li Y, Zhu D, Kippelen B, Marder SR (2007) J Am Chem Soc 129:7246
17. Zhou E, Yamakawa S, Tajima K, Yang C, Hashimoto K (2009) Chem Mater 21:4055
18. Brédas JL (1985) J Chem Phys 82:3808
19. Cheng YJ, Yang SH, Hsu CS (2009) Chem Rev 109:5868

20. Brocks G, Tol A (1996) J Phys Chem 100:1838
21. Hou J, Chen HY, Zhang S, Li G, Yang Y (2008) J Am Chem Soc 130:16144
22. Liang YY, Wu Y, Feng DQ, Tsai ST, Son HJ, Li G, Yu LP (2009) J Am Chem Soc 131:56
23. Park SH, Roy A, Beaupre S, Cho S, Coates N, Moon JS, Moses D, Leclerc M, Lee K, Heeger AJ (2009) Nat Photonics 3:297
24. Patil AV, Lee WH, Kim K, Park H, Kang IN, Lee SH (2011) Polym Chem 2:2907
25. Pomerantz M, Chalonner-Gill B, Harding MO, Tseng JJ, Pomerantz WJ (1992) J Chem Soc Chem Commun 1672
26. Wudl F, Kobayashi M, Heeger AJ (1984) J Org Chem 49:3382
27. Chen GY, Chiang CM, Kekuda D, Lan SC, Chu CW, Wei KH (2010) J Polym Sci A Polym Chem 48:1669
28. Yuan MC, Chiu MY, Liu SP, Chen CM, Wei KH (2010) Macromolecules 43:6936
29. Patil AV, Lee WH, Lee E, Kim K, Kang IN, Lee SH (2011) Macromolecules 44:1238
30. Jung JW, Liu F, Russell TP, Jo WH (2012) Energy Environ Sci 5:6857
31. Lee K, Sotzing GA (2001) Macromolecules 34:5746
32. Sotzing GA, Lee K (2002) Macromolecules 35:7281
33. Lee B, Yavuz MS, Sotzing GA (2006) Macromolecules 39:3118
34. Chen HY, Hou JH, Zhang SQ, Liang YY, Yang GW, Yang Y, Yu LP, Wu Y, Li G (2009) Nat Photonics 3:649
35. Liang Y, Xu Z, Xia J, Tsai ST, Wu Y, Li G, Ray C, Yu L (2010) Adv Mater 22:E135
36. Hou J, Chen HY, Zhang S, Chen RI, Yang Y, Wu Y, Li G (2009) J Am Chem Soc 131:15586
37. Liang Y, Wu Y, Feng D, Tsai ST, Li G, Ray C, Yu L (2009) J Am Chem Soc 131:7792
38. Osaka I, Sauve G, Zhang R, Kowalewski T, McCullough RD (2007) Adv Mater 19:4160
39. Sun Y, Ma Y, Liu Y, Lin Y, Wang Z, Wang Y, Di C, Xiao K, Chen X, Qiu W, Zhang B, Yu G, Hu W, Zhu D (2006) Adv Funct Mater 16:426
40. Sun Y, Liu Y, Ma Y, Di C, Wang Y, Wu W, Yu G, Hu W, Zhu D (2006) Appl Phys Lett 88:242113
41. Li J, Ong KH, Lim SL, Ng GM, Tan HS, Chen ZK (2011) Chem Commun 47:9480–9482
42. Barbarella G, Favaretto L, Sotgiu G, Antolini L, Gigli G, Cingolani R, Bongini A (2001) Chem Mater 13:4112
43. Sotgiu G, Favaretto L, Barbarella G, Antolini L, Gigli G, Mazzeo M, Bongini A (2003) Tetrahedron 59:5083
44. Sotgiu G, Zambianchi M, Barbarella G, Aruffo F, Cipriani F, Ventola A (2003) J Org Chem 68:1512
45. Frey J, Bond AD, Holmes AB (2002) Chem Commun 20:2424
46. He M, Zhang F (2007) J Org Chem 72:442
47. Arbizzani C, Catellani M, Mastragostino M, Cerroni MG (1997) J Electroanal Chem 423:23
48. Catellani M, Lazzarom R, Luzzati S, Brédas JL (1999) Synth Met 101:175
49. Tauc J (1974) Amorphous and liquid semiconductors. Plenum, New York
50. Cervini R, Holmes AB, Moratti SC, Köhler A, Friend RH (1996) Synth Met 76:169
51. Li Y, Xue L, Li H, Li Z, Xu B, Wen S, Tian W (2009) Macromolecules 42:4491
52. Li G, Shrotriya V, Yao Y, Yang Y (2005) J Appl Phys 98:043704/1
53. Li G, Yao Y, Yang H, Shrotriya Y, Yang G, Yang Y (2007) Adv Funct Mater 17:1636
54. Chen LM, Hong Z, Li G, Yang Y (2009) Adv Mater 21:1434
55. Yao Y, Hou J, Xu Z, Li G, Yang Y (2008) Adv Funct Mater 18:1783